Semarak Engineering Journal

Journal homepage:
https://semarakilmu.my/index.php/sej/index
ISSN: 3036-0145

Coupled Thermochemical Mechanism in Plasma Co-Gasification of Empty Fruit Bunches and Plastic Waste: Evaluation of Syngas and Char Microstructural Evolution

Dashvenan Letchumanan[1], Afiq Asmawi[1], Izuan Amin Ishak[2], Rais Hanizam Madon[1], Nik Normunira Mat Hassan[3], Yos Nofendri[4], Nor Afzanizam Samiran[2,*]

[1] Faculty of Mechanical and Manufacturing Engineering, Universiti Tun Hussein Onn Malaysia (UTHM), 86400 Parit Raja, Batu Pahat, Johor, Malaysia
[2] Department of Mechanical Engineering Technology, Faculty of Engineering Technology, Universiti Tun Hussein Onn Malaysia (UTHM) Higher Education Hub Pagoh, KM 1, Jalan Panchor, 84600 Panchor, Johor, Malaysia
[3] Faculty of Mechanical Engineering, Kompleks Kejuruteraan Tuanku Abdul Halim Mu'adzam Shah, Universiti Teknologi MARA, 40450 Shah Alam, Selangor, Malaysia.
[4] Fakultas Teknologi Industri & Informatika, Universitas Muhammadiyah Prof DR Hamka, J. Tanah Merdeka No. 6, RT. 10/ RW. 5, Rambutan, Kec. Ciracas, Kota Jakarta Timur, Daerah Khusus Ibukota Jakarta 13830, Indonesia.

ARTICLE INFO

Article history:
Received 18 May 2026
Received in revised form 24 June 2026
Accepted 26 June 2026
Available online 7 September 2026

ABSTRACT

The increase in the production of municipal solid waste (MSW) and oil palm biomass in Malaysia needs to be managed using more advanced thermochemical solutions to overcome the shortcomings of existing conventional gasification technologies such as high tar production, low conversion efficiency, and unstable syngas quality. This study was conducted to evaluate the performance of a thermal arc plasma co-gasification process using a combination of oil palm empty bunches (EFB) and plastic waste, specifically low-density polyethylene (LDPE) and polyethylene terephthalate (PET) as feedstock. The experiments were conducted in triplicates to ensure data reliability, using a 9 kW plasma integrated downdraft reactor operating at atmospheric pressure with a reaction time of 10–12 minutes at 90/10, 80/20, and 70/30 blend ratios. Gas chromatography analysis revealed that increasing the plastic fraction significantly enhanced hydrogen production (H2), with the EFB-LDPE blend reaching a maximum concentration of 8.83% at the 70/30 ratio, indicating an improvement in syngas quality. The optimum energy yield was obtained at the 80/20 blend ratio, producing a peak high calorific value (HHV) of 3.72 MJ/kg for the LDPE blend and 2.91 MJ/kg for the PET blend, demonstrating favourable energy recovery potential. Scanning Electron Microscopy (SEM) analysis using ImageJ software showed that the incorporation of LDPE increased the porous area to 18.05% with an average pore size of 55.29 μm^2, suggesting enhanced gas-solid interaction and improved char reactivity during the gasification process. In addition, Fourier Transform Infrared Spectroscopy (FTIR) analysis provided evidence at the molecular level regarding the ability of plasma to decompose complex polymer structures. For the EFB-PET char product, the appearance of peaks at 1014.93 cm^{-1} and 1378.04 cm^{-1} indicated the formation of ester bonds and partial decomposition of the polymer

* *Corresponding author.*
E-mail address: afzanizam@uthm.edu.my (Nor Afzanizam Samiran)

https://doi.org/10.37934/sej.16.1.1633

Keywords:
Plasma co-gasification; Hydrogen-rich syngas; Oil palm biomass; Waste-to-energy (WtE); Char characterization; Polymer decomposition

chain. For the EFB-LDPE sample, the detection of C=N stretching vibrations at 2332.52 cm^{-1} and C-O-C ester vibrations at 1012.98 cm^{-1} confirmed the existence of a structural recombination process and strong interactions between the biomass fraction and the polymer. Overall, these findings prove that plasma co-gasification can not only optimize syngas quality, but also assist in the complete transformation of waste into more stable char residue with the presence of distinctive functional groups.

1. Introduction

Municipal solid waste (MSW), often known as solid waste, is produced daily by the industrial and agricultural sectors and is typically disposed of by society. The rise in the global population, along with patterns of urbanization and socioeconomic needs, is resulting in a corresponding surge in the production of solid waste. Global citizens are increasingly concerned with the management of trash. Due to Malaysia's excessive garbage output surpassing its recycling rate, waste management has become a significant concern in the country. Daily, Malaysians dispose of around 30,000 tons of MSW, equivalent to roughly 1.17 kilograms of waste per individual. Transforming waste into syngas or synthesis gas can supplant diminishing natural resources, serving as a substitute for natural gas in industrial and everyday energy uses. For example, syngas can be combusted directly in petrol engines, utilized for the manufacture of methanol and hydrogen, or transformed into synthetic liquid fuel using the Fischer-Tropsch method [1].

In addition to MSW, biomass waste is also regarded as a potential raw material for renewable energy sources. The expansion of palm oil production in Malaysia is paralleled by a rise in the quantity of wastes produced. Presently, Malaysia and Indonesia provide 86.5% of the 57 million tons of global palm oil production [2]. Annually, the palm oil industry in Malaysia generates around 40 million tonnes of oil palm biomass and 50 million tonnes of palm oil mill effluents (POME). The current waste management practices, such as biomass combustion, have adverse environmental effects due to the emission of greenhouse gases and the substantial residual organic matter [3]. The diverse forms of biomass generated, including empty fruit bunches (EFB), oil palm fiber (OPF), oil palm shell (OPS), wet shell, palm kernel, fronds, and trunks, offer a promising prospect for effective use. Gasification can transform oil palm biomass leftovers into syngas, serving as a useful energy source in the industry. The renewable characteristic of oil palm biomass emphasizes its significance as a substantial energy resource in Malaysia.

Gasification is a procedure that involves heating carbonaceous material, whether solid or liquid, with a gasifying agent to produce syngas. Coals and biomass, which are carbonaceous fuels, are frequently employed in gasification processes to generate syngas. The gases produced typically have a low to medium heating value. Combustion is prevented to avoid any remaining heat value in the flue gas resulting from incomplete fuel combustion. The gasification process involves partial oxidation of fuel or fuel-rich combustion, as well as hydrogenation. The selection of an oxidant or gasifying agent, such as steam, carbon dioxide, air, or oxygen, is contingent upon the desired chemical composition and efficiency of the syngas [4]. Operating at high temperatures, the gasification process purifies corrosive ash components, resulting in the generation of clean syngas that is suitable for immediate utilization.

Although traditional gasification is generally regarded as a clean energy method, it also posed a few disadvantages, such as producing tar. The utilization of biomass gasification may give rise to several issues related to the existence of tar, including equipment blockages, diminished system performance, production of substandard gas output, and increased maintenance requirements.

Plasma gasification technology, which operates at atmospheric pressure and rapidly reaches higher temperatures compared to conventional gasifiers, can effectively address these limitations. Plasma gasification, unlike traditional methods, utilizes external electric energy to generate a high-temperature plasma flame, achieving the desired gasification reaction temperature [5]. This method, commonly known as "true gasification" or "pure gasification," facilitates a gasification process with minimal combustion, promoting chemical reactions by producing active particles such as radicals and ions [6]. The higher temperatures in plasma gasification not only enhance the efficiency of the gasification process but also reduce tar formation and other by-products, leading to cleaner syngas production. Thus, plasma gasification emerges as a superior alternative to conventional gasification methods, offering a more efficient and environmentally friendly solution for converting waste into energy.

The feedstock composition during gasification processes has a significant impact on syngas composition, gas output, H_2/CO ratio, and lower heating value (LHV). The studies conducted by Lestander and Pandey et al. have demonstrated that the chemical reactions and equilibrium occurring during gasification are influenced by various factors, including the elemental composition, heating values, flammable substance concentrations, and ash characteristics of the feedstock. Consequently, several elements contribute to this influence [7, 8]. According to Hasanzadeh (2022), feedstocks with a high carbon content can significantly impact the hydrogen concentration in the syngas composition. This was demonstrated in their investigation through the utilisation of coal and plastic waste, which possess a significant amount of carbon, as raw materials for steam co-gasification. The result yielded a syngas with a high concentration of hydrogen. This highlights the importance of considering the composition of the feedstock when attempting to alter the properties of syngas in gasification operations. High-carbon feedstocks, such as plastic waste, can increase the syngas's hydrogen concentration.

Co-gasification is an advanced and promising technique used to convert combinations of different feedstocks into syngas. The composition profile of the feedstock selected in the gasification process essentially plays a very critical role in determining the final quality of the resulting syngas. Therefore, any variation in the characteristics of this feedstock will trigger a chain change in the final composition of the syngas, which directly affects important parameters such as the amount of gas output, the H_2/CO ratio, and the low calorific value (LHV) produced. Referring to the studies by Lestander et al. and Pandey et al., the dynamics of chemical reactions and equilibrium in the reactor are actually greatly influenced by the intrinsic properties of the material including the elemental composition, heating value, and ash characteristics of the feedstock [7, 8]. A more specific point was raised by Hasanzadeh et al., who emphasized that high carbon content is the main factor that can "pull" the hydrogen concentration in syngas to a higher level. This is evidenced by the use of materials such as plastic waste and coal in the steam co-gasification process, whose high carbon content consistently produces hydrogen-rich syngas. This shows that manipulation of feedstock type is not just a technical choice, but a strategy to obtain optimal syngas specifications for industrial purposes [9].

A literature review shows that various conventional thermal approaches have been widely explored for the co-gasification process of biomass and plastic waste. In a downdraft reactor, Fazil et al. found that the addition of 25 wt% low-density polyethylene (LDPE) waste with garden waste biomass successfully increased the syngas heating value, cold gas efficiency, and reduced solid waste (clinker) [10]. Using a low-temperature steam-oxy fluidized bed reactor, Bhattarai et al. concluded that a mixture of HDPE and pine waste produce the highest syngas yield compared to polystyrene which produced high content of tar [11]. For two-stage gasification, Salisu et al. reported that the use of Ni-Fe/CaO-SBA-15 catalyst with rice husk and 75–100% plastic composition was capable of

achieving optimum yield and hydrogen concentration [12]. In terms of the chemical composition of air gasification, Ajorloo et al. found that the various type of biomass (especially high in hemicellulose and lignin) demonstrates a more significant effect on the gas profile than the plastic waste [13]. Meanwhile, a CO2 gasification study by Liu et al. found that PE blends improved the quality of the syngas heating value, while PVC accelerated the rate of wood dust volatilization [14]. At a pilot scale of 100 kg/h, Parrillo et al. demonstrated that varying the plastic-biomass blend ratio and equivalence ratio were drastically resulted on the increased of hydrogen concentration due to the gas-water transfer reaction [15]. Based on this recent literature review, existing studies still rely entirely on conventional thermochemical reactors (such as fluidized bed and fixed bed) which face the challenge of thoroughly removing heavy tar molecules. Therefore, there is a clear research gap where the experimental studies of co-gasification using integration of plasma technology with conventional method which in this case is downdraft reactor to treat mixtures of biomass and plastic waste is rarely investigated.

Although conventional gasification technologies have demonstrated the capability to convert biomass-plastic mixtures into syngas, challenges associated with tar formation, incomplete conversion of heterogeneous feedstocks, and limited understanding of solid residue transformation remain significant. Plasma-assisted gasification offers a potential alternative by providing a high-energy reaction environment capable of promoting secondary cracking reactions and improving feedstock decomposition. In addition, the integration of syngas analysis with detailed char characterization using SEM, porosity analysis, and FTIR enables a more comprehensive understanding of the coupled thermochemical mechanisms occurring during biomass-plastic co-gasification. Hence the present study aims to assess the potential of plasma gasification in producing syngas from the mixtures of LDPE, PET, and EFB.

2. Methodology

2.1 Burner Geometry

The feedstock selected for the co-gasification process in this study are LDPE, PET plastics and EFB pellets. LDPE and PET plastics are derived from abandoned mineral bottles and food packaging plastic, which are randomly collected from residential areas for the experiment. The plastics are then cut into rectangular pieces, each having an area of 1.5cm². The biomass EFB pellets, sourced from Heavy Oil Mill Sdn Bhd, a palm oil processing company situated on the Bahau-Keratong Highway in Mukim Bera, Pahang, have a cylindrical shape with dimensions of 18 mm in length and 8 mm in diameter. These pellets are derived from palm oil palms. The EFB pellets are subjected to proximal examination utilising the LECO TGA- 701 analyzer to determine their physiochemical properties. In addition, the elemental composition of the EFB pellets is analysed using a CHNS/O Analyzer. The information in Table 1 demonstrates a detailed summary of the proximate analysis conducted on Polyethylene terephthalate (PET) and EFB pellets.

LDPE and PET plastics are derived from abandoned mineral bottles and food packaging plastic, which are randomly collected from residential areas for the experiment. The plastics are then cut into rectangular pieces, each having an area of 1.5cm². The biomass EFB pellets, sourced from Heavy Oil Mill Sdn Bhd, a palm oil processing company situated on the Bahau-Keratong Highway in Mukim Bera, Pahang, have a cylindrical shape with dimensions of 18 mm in length and 8 mm in diameter. These pellets are derived from palm oil palms. The EFB pellets are subjected to proximal examination utilising the LECO TGA- 701 analyzer to determine their physiochemical properties. In addition, the elemental composition of the EFB pellets is analyzed using a CHNS/O Analyzer. The information in

Table 3 indicate a detailed summary of the ultimate analyses conducted on Polyethylene terephthalate (PET) and EFB pellets.

Fig. 1. EFB pellet (left), Polyethylene terephthalate (PET) (middle), Low-density polyethylene (LDPE) (right)

Table 2 shows the results of the bomb calorimeter analysis for EFB pellets, PET plastics, and LDPE plastics. The higher calorific values for PET (22378 J/g) and LDPE (19845 J/g) compared to EFB pellets (17219 J/g) indicate that plastics have higher energy content, making them effective for co-gasification processes aimed at energy production. Table 3 presents the ultimate analysis, showing the elemental composition of PET, EFB, and LDPE. The high carbon content in LDPE (84.60%) and PET (62.21%) highlights their significant energy potential. EFB, with a lower carbon content (43.61%) and higher hydrogen content (9.88%), offers a balanced composition for co-gasification. The presence of other elements, including nitrogen and sulfur, in small quantities across the samples, is also noted, which can influence the gasification process and the formation of by-products

Table 1
Proximate analysis of PET plastics and EFB pellets

Sampel	PET (wt%)	LDPE (wt%)	EFB (wt%)
Moisture Content	0.731	0.58	8.683
Volatile Matter	98.726	99.2	70.663
Fixed Carbon	-	-	17.827
Ash Content	0.543	0.22	2.827

Table 2
Characteristics of PET plastics and EFB pellets

Type of sample	HHV (J/g)
EFB Pellet	17219 J/g
Plastic bottle (PET)	22378 J/g
Milo plastic (LDPE)	19845 J/g

Table 3
Ultimate analysis of PET plastics and EFB pellets

Sampel	PET (wt%)	LDPE (wt%)	EFB (wt%)
Weight (mg)	1.949	1.645	2.014
Carbon, C	62.21	43.61	84.60
Hydrogen, H	3.71	9.88	14.30
Nitrogen, N	0.06	0.80	0.00
Sulphur, S	0.16	0.67	0.00
Others	33.86	45.04	1.10

2.2 Instrument

A crucial aspect for achieving a successful experiment is the implementation of a thoroughly and carefully designed study approach of plasma co-gasification system as depicted Figure 2. The initial sample for this study consists of a mixture containing 90% EFB pellet (100g) and 10% PET waste feedstock (900g). To maintain a consistent feedstock weight of 1 kg throughout the experiment, the resulting mixture is then placed into a downdraft gasifier. A suction blower is employed to allow the delivery of air to the gasifier through a pipeline. The frequency controller was set to 16 Hz to enables a precise regulation of the airflow velocity.

An electrical supply is used to activate a 9kW plasma generator, which then generates a plasma flame jet. The purification process of syngas has two serial stages, including removal of particulates using a cyclone filter, followed by temperature reduction of the gas through a condenser, and finally, filtration using an oil and coal filter. The purified syngas is eventually separated into two streams: one is sent towards flare units, while the other is directed towards peristaltic pumps. To assess the flammability of the gas, it is burned using a gas lighter cannon. To minimize the risk of syngas contamination, a cleaning unit that consists of a gas washing bottle (impinger train) is implemented, and peristaltic pumps are also employed to ensure a consistent flow of syngas into the sampling bag.

A gas lighter cannon is utilised to detect the existence of combustible gas by lighting the exit vent of the gas that is released. Subsequently, the syngas should be collected in sample bags in order to facilitate the analysis of its composition using gas chromatography (GC). Three specimen bags are collected throughout each trial, which has a duration of 10 to 12 minutes. To ensure data reliability and reproducibility, all co-gasification runs and sample characterizations were performed in triplicates (n = 3), and the results are reported as the mean values accompanied by their respective standard deviations ($\pm$SD).

After the gasification process is complete, the remaining ash from each specimen is carefully collected. This ash is then analyzed to determine its composition using several techniques, including Scanning Electron Microscopy (SEM), where this technique is used to examine the surface morphology and microstructure of the ash, and Fourier-Transform Infrared Spectroscopy (FTIR), where this method is employed to identify the chemical bonds and molecular structure within the ash. These analyses provide a comprehensive understanding of the by-products of the gasification process and contribute to the optimization and improvement of the overall system.

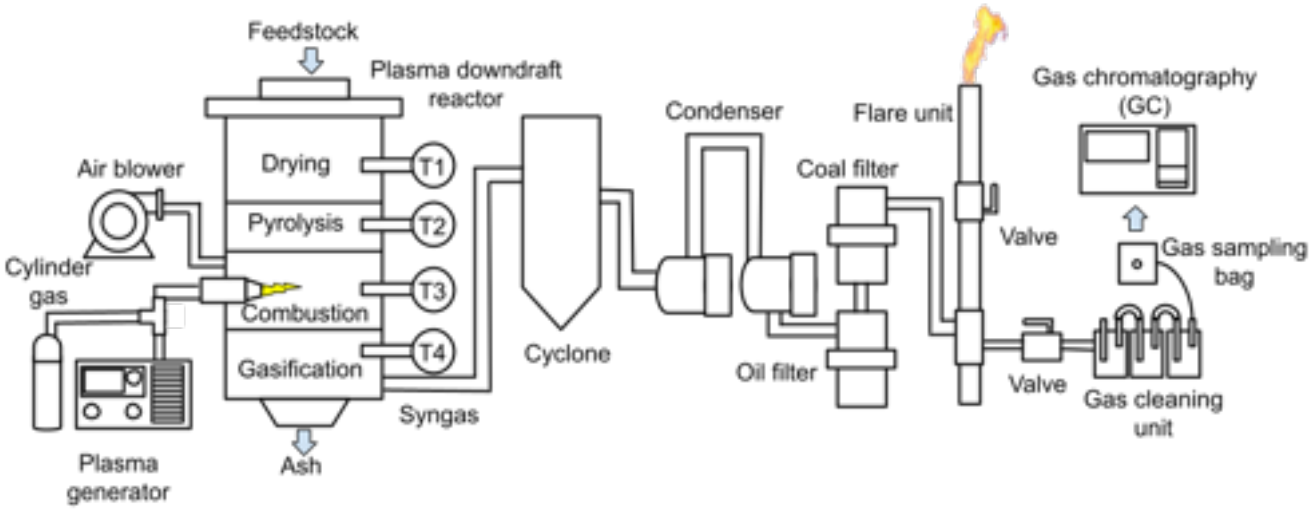

Fig. 2. Schematic flow diagram of plasma downdraft gasification system with cleaning and sampling unit

2.3 Char collection

In addition to syngas analysis, this study also includes in-depth characterization of the solid residue to understand the overall impact of the plasma reaction on the raw material. As shown in Figure 3, the solid residue collected from the ash tray shows a physical appearance of a deep black color with a sandy (granular) texture. This physical appearance suggests that the high carbon content resulting from the thermal decomposition process in the plasma reactor is presence. To understand the characteristics of this residue in more depth, the sample will undergo a series of laboratory analyses such as SEM, FTIR and porosity analysis. SEM is carried out to examine the surface morphology of the granular char microscopically. Porosity analysis is carried out to measure the level of porosity and surface area of the black particles. FTIR is carried out to identify the chemical functional groups that still remain on the char structure.

Fig. 3. Char collected from ash tray after plasma gasification process

2.4 Ash Characterization Techniques

2.4.1 Scanning Electron Microscopy (SEM)

Figure 4 shows the process of preparing the sample and conducting SEM analysis. This analysis was first conducted with sample preparation, during which char samples were dried to eliminate residual moisture. The samples were then mounted on SEM stubs using conductive adhesive tape, followed by sputter-coating with a thin layer of gold to enhance conductivity using SEM coating system. Morphological characteristics of the char were then observed using a scanning electron microscope. High-resolution images were captured to study the surface structure and particle size distribution.

2.4.2 Fourier Transform Infrared Spectroscopy (FTIR) FTIR Analysis

FTIR spectra of the char samples were recorded using an FTIR spectrometer. Spectra were collected in the range of 4000 to 400 cm^{-1}. The functional groups and chemical bonds present in the char were identified by analyzing characteristic absorption bands.

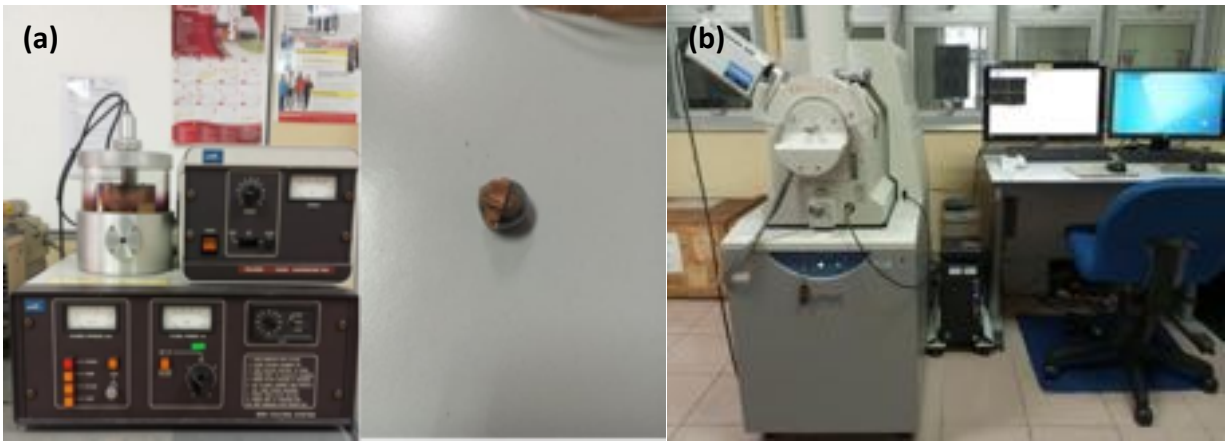

Fig. 4. (a) Sample preparation for SEM analysis (b) SEM analysis using HITACHI-SU 1510

3. Results

3.1 Syngas composition analysis

Figure 5 and Figure 6 shows the results obtained from the thermal arc plasma co- gasification of EFB-LDPE and EFB-PET biomass mixtures. The objective is to analyze the syngas composition and higher heating value (HHV) at different blending ratios (90/10, 80/20, and 70/30). The insights derived from this analysis will aid in understanding the efficiency and viability of using these feedstocks for energy production. The syngas produced from both LDPE-EFB and PET-EFB mixtures demonstrates distinct trends in gas composition across varying blending ratios. Key gases analyzed include hydrogen (H_2), oxygen (O_2), nitrogen (N_2), carbon monoxide (CO), methane (CH_4), and carbon dioxide (CO_2). Additionally, the occurrence of back pressure during the gasification process was observed, which may impact the syngas composition and overall efficiency.

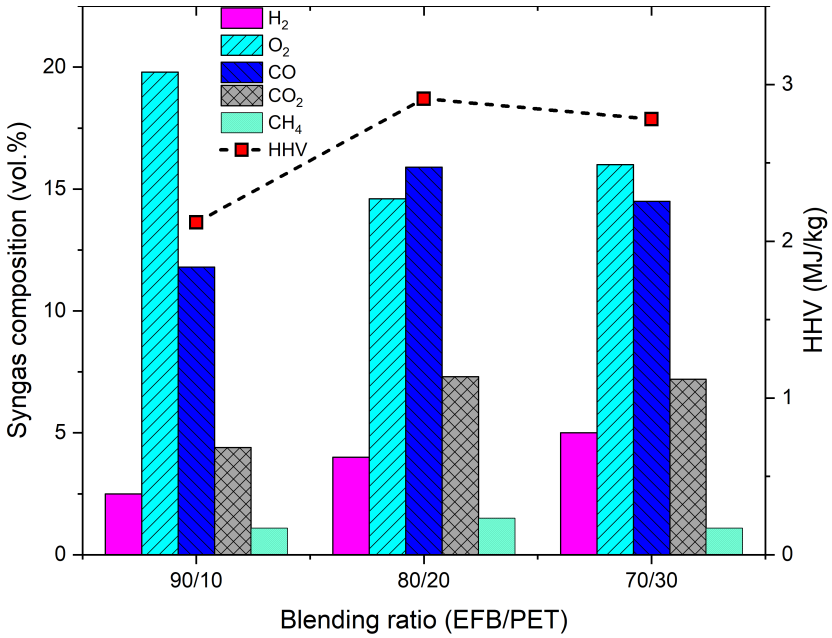

Fig. 5. GC result of gas composition and HHV against EFB/PET blending feedstock

The hydrogen content increases with a higher plastic ratio in both EFB-LDPE and EFB-PET mixtures. Specifically, EFB-LDPE exhibits a more pronounced increase, reaching up to 8.83% ± 0.42% at a 70/30 ratio. This trend indicates that increasing the proportion of LDPE enhances hydrogen production, contributing positively to syngas quality since hydrogen is one of the most desirable combustible components in syngas. The increase in hydrogen concentration suggests that greater plastic incorporation promotes additional thermal cracking and gas-phase reactions during plasma-assisted co-gasification, thereby improving the gaseous fuel characteristics of the product syngas[16]. Oxygen content decreases as the plastic ratio increases, with EFB-LDPE showing a drop from 16.66% ± 0.51% to 13.37% ± 0.45% and EFB-PET from 19.76% ± 0.62% to 15.96% ± 0.48%. The reduction in oxygen content suggests a higher degree of combustion or oxidation of the biomass-plastic mixture, leading to more complete gasification (Hassan et al., 2019). Nitrogen levels remain relatively stable around 74-77% for both feedstocks. This consistency is expected due to the inert nature of nitrogen in the gasification process, which acts as a diluent and influences the overall gas composition [17]. EFB-LDPE shows a slight decrease in CO content from 18.76% ± 0.55% to 16.79% ± 0.52%, whereas EFB-PET exhibits an increase from 11.73% ± 0.38% to 14.46% ± 0.43%. The higher CO content in EFB-PET at increased plastic ratios suggests a more efficient breakdown of the plastic component into CO, potentially enhancing the syngas calorific value [16]. Methane content remains relatively low and stable across all blending ratios for both mixtures. The minimal variation in CH_4 content indicates that the gasification process effectively limits methane production, which is advantageous for reducing greenhouse gas emissions [18]. CO_2 content increases with higher plastic ratios, with EFB-LDPE showing a rise from 5.20% ± 0.22% to 6.13% ± 0.25% and EFB-PET from 4.32% ± 0.18% to 7.23% ± 0.29%. This increase is attributed to the enhanced oxidation of the biomass and plastic components, leading to more complete gasification.

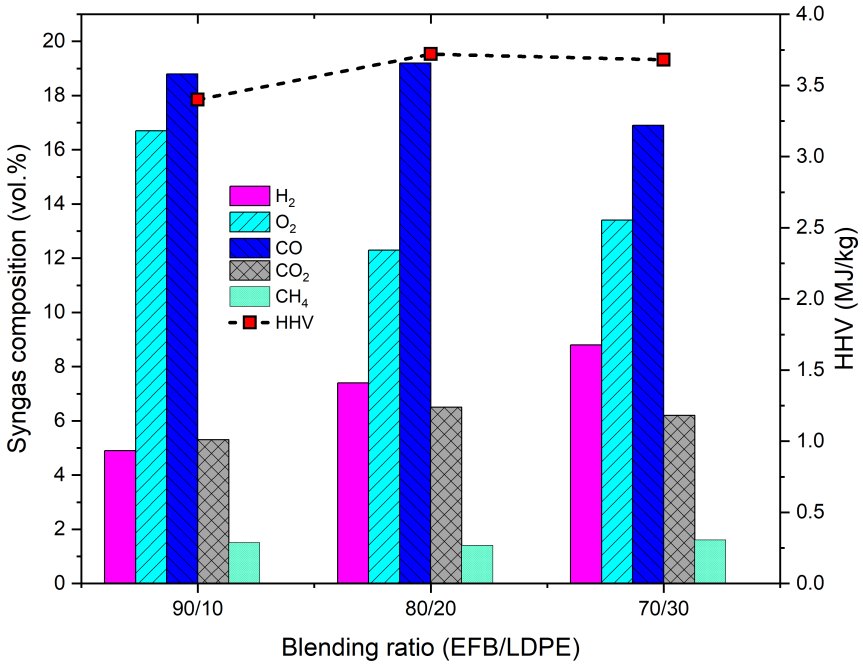

Fig. 6. GC result of gas composition and HHV against EFB/LDPE blending feedstock

The HHV of the syngas is a critical parameter in assessing its energy potential. For EFB-LDPE, the HHV increases from 3.40 ± 0.12 MJ/kg at a 90/10 ratio to 3.72 ± 0.15 MJ/kg at 80/20, followed by a slight decrease to 3.68 ± 0.11 MJ/kg at 70/30. Similarly, EFB-PET shows an increase from 2.13 ± 0.08 MJ/kg to 2.91 ± 0.10 MJ/kg, then a slight decrease to 2.77 ± 0.09 MJ/kg. The higher HHV in EFB-LDPE indicates its superior energy content compared to EFB-PET. The peak HHV at an 80/20 ratio for both mixtures suggests an optimal blending ratio for maximizing energy output. The slight decrease at 70/30 could be due to the dilution effect of excessive plastic, which might not completely gasify, thereby reducing the overall energy content [19]. During the gasification process, back pressure was observed, which could influence the syngas composition and efficiency of the gasification. Back pressure can affect the flow dynamics within the reactor, potentially leading to variations in gas residence time and reaction kinetics, thus impacting the overall gasification performance.

The superior HHV observed at the 80/20 blend ratio suggests that this composition provides a favourable balance between biomass and plastic-derived gaseous products. While increasing the plastic fraction enhanced hydrogen production, the highest hydrogen concentration recorded at the 70/30 ratio did not correspond to the highest HHV. This observation indicates that syngas energy content is influenced by the overall gas composition rather than hydrogen concentration alone. Therefore, the 80/20 blend ratio can be considered an optimum condition for energy recovery, as it achieved the highest HHV while maintaining favourable syngas quality.

In summary, EFB-LDPE outperforms EFB-PET in terms of hydrogen production and HHV, making it a more efficient and potent feedstock for syngas production. However, EFB-PET shows a higher CO content at increased plastic ratios, which could be beneficial for specific industrial applications requiring higher CO levels. These results highlight the potential of using EFB-LDPE and EFB-PET mixtures for syngas production through thermal arc plasma co-gasification, providing valuable insights for optimizing energy output and improving the efficiency of the gasification process.

Compared to conventional gasification systems, the plasma-assisted reactor employed in this study provides a high-energy environment that facilitates the cracking of heavy hydrocarbons and

promotes more extensive feedstock decomposition. While syngas composition is influenced by multiple operating parameters and feedstock characteristics, plasma integration offers additional advantages in terms of reaction intensity and the capability to process heterogeneous biomass-plastic mixtures. Furthermore, the combined evaluation of syngas composition, char morphology, porosity development, and chemical functional groups provides a broader understanding of the thermochemical transformations occurring during the co-gasification process.

3.2 Evaluation of reactivity using the Scanning Electron Microscopy (SEM)

SEM images were analyzed to determine morphological features, including porosity, surface texture, and particle size. Image analysis software (ImageJ) was used for quantitative measurements. The porosity data obtained from the scanning electron microscopy (SEM) analysis of EFB-polymer composites after plasma gasification shows significant differences in both pore size and porosity among different blending ratios of EFB with LDPE and PET, as shown in Figure 7 and Table 4. The distinctions regarding the quality and productivity of syngas generated via plasma gasification have important significance.

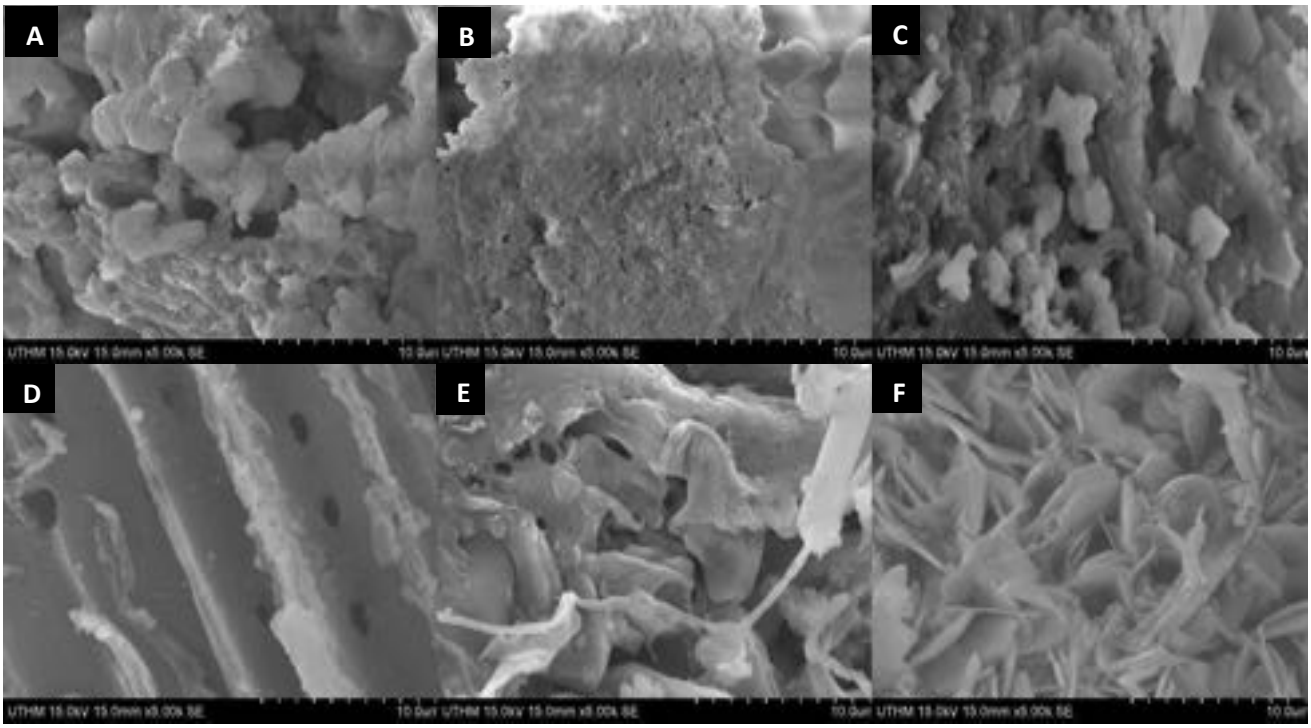

Fig. 7. SEM result for (a) LDPE10% - EFB90%, (b) LDPE20% - EFB80%, (c) LDPE30% - EFB70%, (d) PET10% - EFB 90%, (e) PET20% - EFB80% and (f) PET30% - EFB70%

The porosity characteristics of the ash derived from EFB-LDPE and EFB-PET biomass mixtures were analyzed using SEM (Scanning Electron Microscopy) images processed with ImageJ software. The SEM analysis was conducted to investigate the microstructural characteristics of the ash residues from the gasification process. Understanding the porosity and pore size distribution is essential because it directly influences the reactivity and efficiency of the gasification process. Higher porosity and larger pore sizes can enhance gas flow and reaction rates, leading to more efficient conversion of the feedstock into syngas [20]. The samples were evaluated based on their blend ratios and included the percentage of porous area, mean pore size, and maximum pore size. The results showed significant differences between the two types of mixtures.

For EFB-LDPE samples, the porous area and mean pore size generally increased with higher LDPE content. Sample A (LDPE10%-EFB90%) had a porous area of 16.11% and a mean pore size of 38.42 μm², while Sample C (LDPE30%-EFB70%) showed the highest porous area of 18.05% and a mean pore size of 55.29 μm². This suggests that LDPE contributes to larger and more numerous pores, possibly due to its thermoplastic nature, which may enhance gasification by providing better gas flow paths. The larger pores observed in EFB-LDPE samples correlate with the increased hydrogen production and higher HHV, as better gas flow and enhanced reactivity facilitate more efficient gasification.

In contrast, EFB-PET samples exhibited a different trend. Sample D (PET10%- EFB90%) had a porous area of 10.61% and a mean pore size of 30.48 μm². Interestingly, Sample F (PET30%-EFB70%) showed a decrease in porous area to 7.95% but an increase in mean pore size to 76.32 μm². This indicates that while PET may form fewer pores, these pores are significantly larger, which could affect the uniformity and efficiency of the gasification process. The larger mean pore sizes in PET-EFB samples may explain the higher CO content observed, as larger pores could facilitate the breakdown of PET into CO, enhancing the syngas calorific value [21].

Table 4
Porosity analysis through the pore size evaluation based on SEM Image

Sampel	Blend Ratio	Porous Area (%)	Mean Pore Size (μm²)	Max Pore Size (μm²)
A	LDPE10% - EFB90%	16.11 ± 0.65	38.42 ± 1.55	75
B	LDPE20% - EFB80%	13.90 ± 0.48	43.64 ± 1.82	85
C	LDPE30% - EFB70%	18.05 ± 0.72	55.29 ± 2.10	95
D	PET10% - EFB90%	10.61 ± 0.39	30.48 ± 1.15	80
E	PET20% - EFB80%	15.45 ± 0.58	37.01 ± 1.44	75
F	PET30% - EFB70%	7.95 ± 0.31	76.32 ± 2.95	85

These differences in pore morphology could influence the reactivity and efficiency of the gasification process. Higher porosity and larger pore sizes in EFB-LDPE samples suggest better gas flow and potentially more efficient gasification. In contrast, the larger but fewer pores in EFB-PET samples might impact the uniformity of the gasification process. Future studies should further investigate the impact of these morphological differences on the gasification efficiency and the quality of the syngas produced. Additionally, exploring the underlying mechanisms driving these variations can provide deeper insights into optimizing the gasification process for different biomass-plastic mixtures (Zulkafli et al., 2023).

The development of a more porous char structure is beneficial for gasification performance because it increases the available surface area for gas-solid interactions and facilitates mass transfer within the carbon matrix. Higher porosity generally indicates a greater degree of feedstock decomposition and structural transformation during the gasification process. Therefore, the observed increase in porous area and pore size, particularly for the LDPE-containing samples, suggests enhanced char reactivity and improved accessibility of reactive sites during plasma-assisted co-gasification.

3.3 Fourier Transform Infrared Spectroscopy (FTIR) analysis

FTIR spectra were analyzed to identify functional groups present in the char. Peak assignments were made based on Characteristic IR Band Positions tables. The plasma gasification process, which utilizes high-temperature ionized gas (plasma) to decompose organic materials, converts complex

polymers and biomass into simpler gases, known as syngas, along with other byproducts. This high-energy process significantly alters the chemical structure of the materials, and the resultant changes can be studied using Fourier Transform Infrared Spectroscopy (FTIR). FTIR helps identify functional groups and characterize chemical bonds within the samples by measuring the absorbance of various infrared frequencies.

The FTIR analysis of EFB-PET samples post-plasma gasification indicates significant structural and chemical modifications as shown in Figure 8. For the PET10%-EFB90% sample, characteristic peaks at 2974.22cm^{-1} (C-H stretching vibrations in CH_2 or CH_3 groups) and 1571.99cm^{-1} (C=C stretching vibrations) suggest the retention of some polymeric structures. The presence of peaks at 1460.36cm^{-1} (CH_2 bending vibrations) and 1347.87cm^{-1} (CH_3 bending vibrations) indicates minor structural changes. Peaks at 980.2cm^{-1} (C-OH stretching vibrations) and 614.93cm^{-1} (out-of-plane bending vibrations) imply partial decomposition and interaction with EFB [22]. In the PET20%-EFB80% sample, peaks at 2972.76cm^{-1} (C-H stretching vibrations) and 1569.96cm^{-1} (C=C stretching vibrations) indicate that the polymeric nature is somewhat preserved. The peak at 1378.04cm^{-1} (CH_3 bending vibrations) and 1014.93cm^{-1} (C-O-C vibrations in esters) point towards the formation of ester linkages or partial breakdown products [23]. For the PET30%-EFB70% sample, the peak at 3677.03cm^{-1} indicates OH stretching vibrations (free OH), likely from the EFB. Peaks at 2972.24cm^{-1} (C-H stretching vibrations) and 1570.02cm^{-1} (C=C stretching vibrations) reflect similar structural components. Additional peaks at 1385.31cm^{-1} (CH_3 bending vibrations), 874.96cm^{-1} ($C=CH_2$ out-of-plane bending vibrations), 822.01cm^{-1} (possibly C-H out-of-plane bending vibrations), 744.38cm^{-1}, and 694.95cm^{-1} (both CH=CH-(cis) out-of-plane bending vibrations) indicate significant structural changes and the formation of new chemical environments [24].

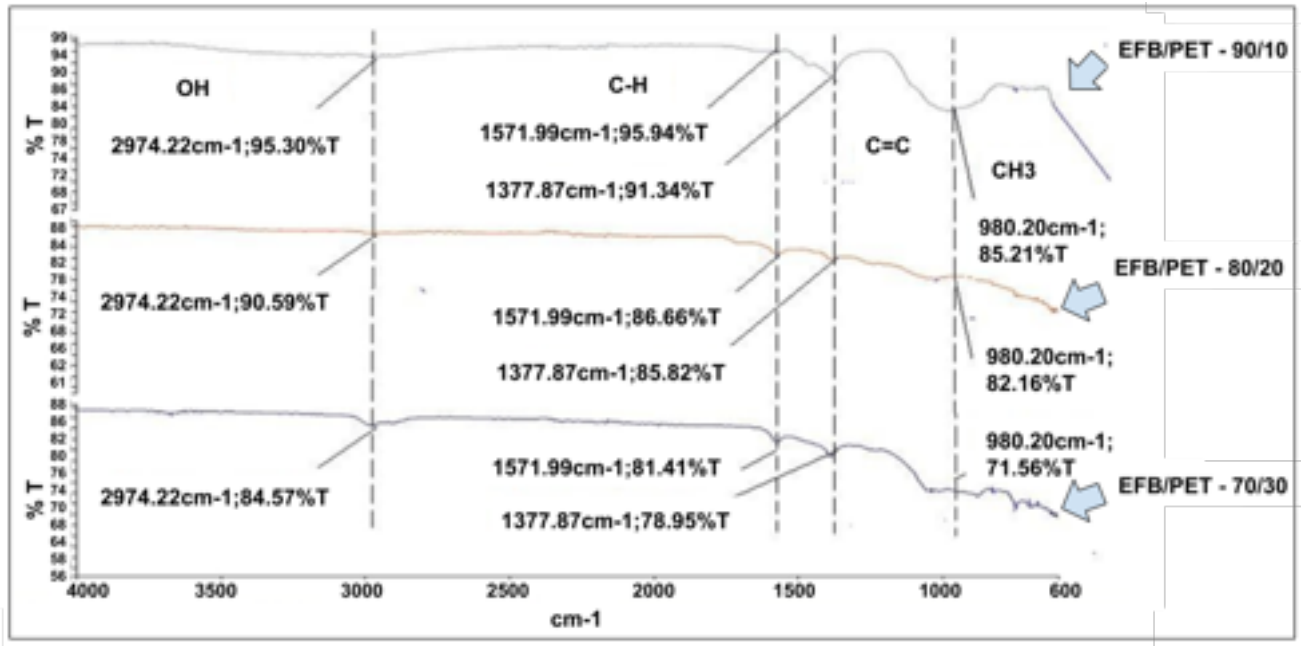

Fig. 8. FTIR result for EFB/PET blending feedstock

The FTIR analysis of EFB-LDPE samples also reveals substantial chemical transformations as shown in Figure 9. For the LDPE10%-EFB90% sample, the peak at 3207.92cm^{-1} corresponds to OH stretching vibrations (intermolecular H bonds), while the peak at 2332.52cm^{-1} indicates C≡N stretching vibrations (nonconjugated). Peaks at 1641.71cm^{-1} and 1570.16cm^{-1} (C=C stretching vibrations) reflect the retention of some double bonds. The presence of peaks at 1376.57cm^{-1} (CH_3 bending vibrations), 984.64cm^{-1} (C-OH stretching vibrations), and 743.03cm^{-1} (CH=CH-(cis) out-of-plane bending

vibrations) suggests hydrogen bonding and partial decomposition (Armenise et al., 2021). In the LDPE20%-EFB80% sample, the peak at 1570.21cm^{-1} (C=C stretching vibrations) and 1377.17cm^{-1} (CH_3 bending vibrations) indicate the breakdown of LDPE and interaction with EFB. The peak at 1012.98cm^{-1} (C-O-C vibrations in esters) suggests the formation of esters (Liu et al., 2021). For the LDPE30%-EFB70% sample, peaks at 3127.01cm^{-1} (OH stretching vibrations), 2321.84cm^{-1} (C≡N stretching vibrations), and 1570.95cm^{-1} (C=C stretching vibrations) show the formation of new functional groups. Additional peaks at 1459.18cm^{-1} (CH_2 bending vibrations), 1377.51cm^{-1} (CH_3 bending vibrations), 990.71cm^{-1} (C-O-C vibrations in esters), and 862.17cm^{-1} ($CH=CH_2$ out-of-plane bending vibrations) suggest significant structural changes and interactions between LDPE and EFB [25].

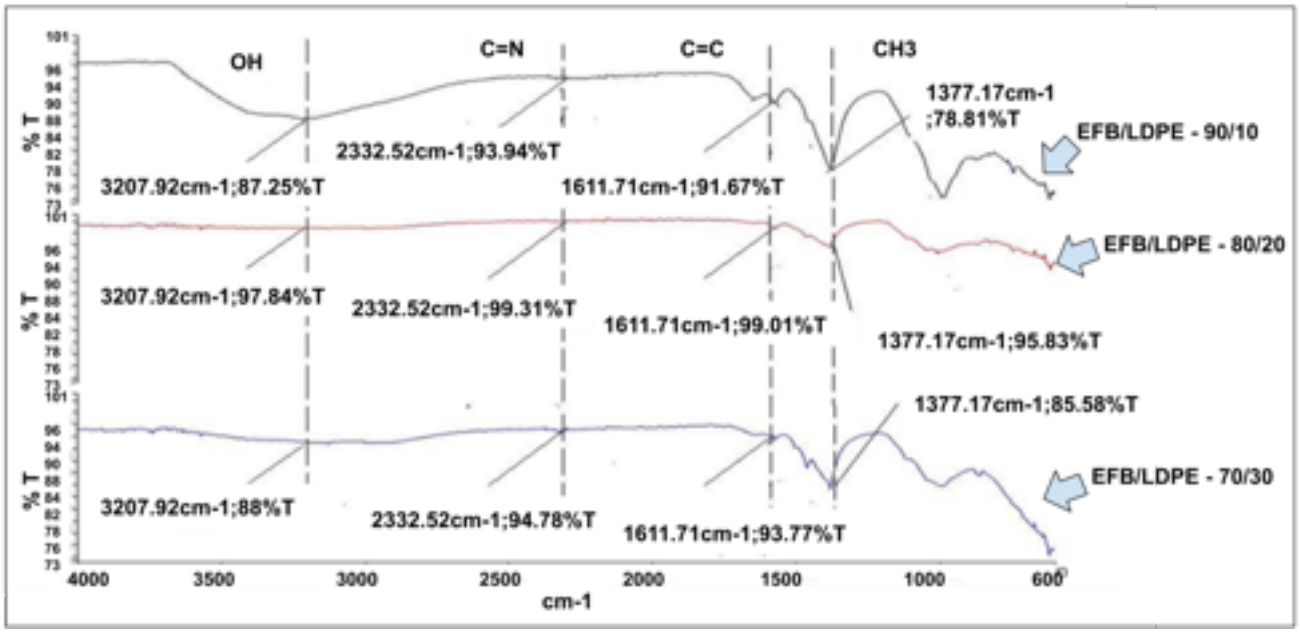

Fig. 9. FTIR result for EFB/LDPE blending feedstock

The FTIR analysis of both EFB-PET and EFB-LDPE samples post-plasma gasification reveals the presence of various functional groups such as OH, C-H, C=C, CH_2, CH_3, C≡N, and C-O-C. These functional groups indicate partial decomposition of the original polymers and the formation of new chemical bonds due to the high-energy plasma environment. The variations in transmittance (%T) values reflect different degrees of interaction or changes in the chemical environment, highlighting the complex chemical transformations occurring during the gasification process. This understanding is crucial for optimizing the plasma gasification process to enhance syngas yield and quality.

The differences in peak values between different ratios of PET-EFB and LDPE-EFB samples are primarily due to the varying compositions of the materials. Higher EFB content leads to more significant contributions from the cellulose, hemicellulose, and lignin present in the EFB, which introduces new functional groups such as OH and C-O-C. Conversely, higher PET or LDPE content retains more of the polymeric structure, reflected in the presence of C-H, C=C, and CH_2/CH_3 groups. Additionally, the interaction between the polymer and EFB components during the plasma gasification process results in different degrees of decomposition and recombination, leading to variations in the observed FTIR peaks. The specific environment and the chemical nature of each component influence the formation and intensity of the detected functional groups, thus explaining the differences in peak values across different sample ratios.

4. Conclusions

This study demonstrates the potential of integrating plasma technology with a downdraft reactor for the co-gasification of biomass and plastic waste. The plasma-assisted process provides a high-energy reaction environment that promotes feedstock decomposition and offers potential advantages in addressing challenges commonly associated with conventional gasification systems, particularly when processing heterogeneous biomass-plastic mixtures.

The experimental results also revealed that the optimum blending ratio depends on the performance indicator being considered. Although the highest hydrogen concentration was obtained at the 70/30 blend ratio, the maximum HHV was achieved at the 80/20 ratio for both LDPE and PET mixtures. This observation suggests the existence of a performance trade-off, where further increases in plastic content may favour hydrogen generation but do not necessarily translate into higher overall syngas energy content. Therefore, the 80/20 blend ratio represents a more balanced condition for maximizing energy recovery while maintaining favourable syngas composition. Based on the results of the study, several important conclusions can be formulated as follows:

- Syngas Optimization: Hydrogen gas production (H_2) shows a significant increase trend along with the increase in plastic ratio, where the EFB-LDPE mixture recorded the highest concentration of 8.83% at a ratio of 70/30. In addition, the 80/20 mixture ratio was identified as the best configuration to maximize the energy potential (HHV) for both types of samples with peak values of 3.72 MJ/kg for LDPE and 2.91 MJ/kg for PET, respectively.
- The superior HHV achieved at the 80/20 blend ratio indicates that optimum gasification performance is not solely dependent on maximizing hydrogen concentration. Instead, the results suggest that an appropriate balance between biomass and plastic content is required to maximize overall syngas energy recovery. Consequently, the 80/20 blend ratio was identified as the optimum operating condition within the investigated range.
- Microstructural Evolution: SEM analysis results confirmed that the thermoplastic nature of LDPE helps to form a more porous char structure, with a maximum porous area reaching 18.05%. The presence of these larger pores directly helps to improve the gas flow path and increase the level of reactivity throughout the gasification process.
- Evidence of Chemical Transformation: FTIR analysis successfully provided strong evidence at the molecular level on the ability of high-energy plasma environment to decompose complex polymer structures. For the EFB-PET sample, the appearance of peaks at 1014.93 cm^{-1} and 1377.87 cm^{-1} indicated the formation of ester bonds and partial decomposition of the polymer chain. Meanwhile, for the EFB-LDPE sample, the detection of C=N stretching vibrations at 2332.52 cm^{-1} confirmed the existence of a structural recombination process and strong chemical interactions between the biomass fraction and the polymer.
- Environmental Impact: Overall, the findings demonstrate the potential of plasma-assisted co-gasification as a thermochemical conversion approach for the valorisation of municipal solid waste (MSW) and palm oil agricultural waste in Malaysia through the production of syngas as a potential energy carrier.

Despite the promising findings obtained in this study, several limitations should be acknowledged. The experiments were conducted using a laboratory-scale plasma-assisted downdraft gasification system, and therefore the observed performance may differ under industrial-scale operating conditions. In addition, only selected EFB-plastic blending ratios were investigated, whereas variations in feedstock composition and properties may influence gasification behaviour and

syngas quality. The present study also focused primarily on syngas composition and char characteristics and did not include detailed evaluation of plasma energy consumption, reactor durability, or long-term operational stability. Therefore, future studies should address these aspects to further assess the technical feasibility and practical implementation of plasma-assisted co-gasification systems.

The findings of this study contribute to addressing the research gaps identified in the Introduction regarding the thermochemical behaviour of heterogeneous EFB-plastic mixtures under plasma-assisted gasification conditions. The observed increase in hydrogen production demonstrates the feasibility of converting mixed biomass-plastic feedstocks into combustible gaseous products, while the SEM and FTIR analyses provide additional insight into char evolution and chemical transformation mechanisms. These findings expand the current understanding of biomass-plastic co-gasification and provide experimental evidence on the influence of feedstock composition on syngas quality and char characteristics in plasma-assisted gasification systems.

Acknowledgement
This research was supported by Universiti Tun Hussein Onn Malaysia (UTHM) through TIER 1 (vot J116).

Conflict of Interest Statement
The authors declare that there is no conflict of interest regarding the publication of this paper. No financial support, grants, or other forms of compensation were received that could have influenced the outcomes of this work. The research was conducted in the absence of any commercial or financial relationships that could be construed as a potential conflict of interest.

Author Contributions Statement
Dashvenan Letchumanan and Afiq Asmawi conducted the experimental investigations, performed data analysis, and wrote the initial draft of the manuscript. Nor Afzanizam Samiran designed the study, supervised the project, and reviewed the manuscript. Izuan Amin Ishak, Rais Hanizam Madon, and Nik Normunira Mat Hassan contributed to data interpretation and manuscript revision. All authors have read and approved the final version of the manuscript.

Data Availability Statement
All data generated or analyzed during this study are included in this published article. Additional datasets regarding the numerical simulations are available from the corresponding author upon reasonable request.

Ethics Statement
This study was conducted in accordance with the ethical standards of the institutional and national research committee. As this research involved numerical modeling and simulation, no human or animal participants were involved, and informed consent was not required.

References
[1] Speight, James G. "Recovery, Storage, and Transportation." In *Natural Gas*, 149-86, 2019.
[2] Noirot, L. M., D. S. Muller-Stover, R. Wahyuningsih, H. Sorensen, Sudarno, A. Simamora, Pujianto, Suhardi, and J. P. Caliman. "Impacts of Empty Fruit Bunch Applications on Soil Organic Carbon in an Industrial Oil Palm Plantation." *J Environ Manage* 317 (Sep 1 2022): 115373. https://doi.org/10.1016/j.jenvman.2022.115373. https://www.ncbi.nlm.nih.gov/pubmed/35649336.

[3] Yaman, Cevat. "Investigation of Greenhouse Gas Emissions and Energy Recovery Potential from Municipal Solid Waste Management Practices." *Environmental Development* 33 (2020). https://doi.org/10.1016/j.envdev.2019.100484.

[4] Yaashikaa, P. R., P. S. Kumar, S. Varjani, and A. Saravanan. "A Critical Review on the Biochar Production Techniques, Characterization, Stability and Applications for Circular Bioeconomy." *Biotechnol Rep (Amst)* 28 (Dec 2020): e00570. https://doi.org/10.1016/j.btre.2020.e00570. https://www.ncbi.nlm.nih.gov/pubmed/33304842.

[5] Zeng, Yimin, and Xue Han. "Co-Processing Biomass with Fossil Fuels." In *Encyclopedia of Renewable Energy, Sustainability and the Environment*, 731-44, 2024.

[6] Cortazar, M., L. Santamaria, G. Lopez, J. Alvarez, L. Zhang, R. Wang, X. Bi, and M. Olazar. "A Comprehensive Review of Primary Strategies for Tar Removal in Biomass Gasification." *Energy Conversion and Management* 276 (2023). https://doi.org/10.1016/j.enconman.2022.116496.

[7] Lestander, Torbjörn A., Fredrik Weiland, Alejandro Grimm, Magnus Rudolfsson, and Henrik Wiinikka. "Gasification of Pure and Mixed Feedstock Components: Effect on Syngas Composition and Gasification Efficiency." *Journal of Cleaner Production* 369 (2022). https://doi.org/10.1016/j.jclepro.2022.133330.

[8] Pandey, Preeti H., Tejas M. Ukarde, Jyoti S. Mahale, Ayush Vasishta, and Hitesh S. Pawar. "Syngas Production Via Biomass Gasification." In *Biomass, Biofuels, Biochemicals*, 211-61, 2022.

[9] Hasanzadeh, Rezgar, Parisa Mojaver, Ata Chitsaz, Mehran Mojaver, Mohammad Jalili, and Marc A. Rosen. "Biomass and Low-Density Polyethylene Waste Composites Gasification: Orthogonal Array Design of Taguchi Technique for Analysis and Optimization." *International Journal of Hydrogen Energy* 47, no. 67 (2022): 28819-32. https://doi.org/10.1016/j.ijhydene.2022.06.244.

[10] Fazil, A., Sandeep Kumar, and Sanjay M. Mahajani. "Downdraft Co-Gasification of High Ash Biomass and Plastics." *Energy* 243 (2022). https://doi.org/10.1016/j.energy.2021.123055.

[11] Bhattarai, A., H. Khodaei, and S. Adhikari. "Oxy-Steam Fluidized Bed Co-Gasification of Plastic Wastes and Biomass: Experimental Study and Cfd Simulation." *Waste Manag* 204 (Aug 1 2025): 114931. https://doi.org/10.1016/j.wasman.2025.114931. https://www.ncbi.nlm.nih.gov/pubmed/40482581.

[12] Salisu, Jamilu, Ningbo Gao, Cui Quan, Jale Yanik, and Norbert Miskolczi. "Hydrogen-Rich Syngas Production Via Two-Stage Co-Gasification of Biomass and Plastic Using a Novel Ni-Fe/Cao-Sba-15 Catalyst: Experimental Study and Ann-Based Prediction." *Process Safety and Environmental Protection* 198 (2025). https://doi.org/10.1016/j.psep.2025.107199.

[13] Ajorloo, Mojtaba, Maryam Ghodrat, Jason Scott, and Vladimir Strezov. "Experimental Analysis of the Effects of Feedstock Composition on the Plastic and Biomass Co-Gasification Process." *Renewable Energy* 231 (2024). https://doi.org/10.1016/j.renene.2024.120960.

[14] Liu, Qian, Jianguo Sun, Yonghua Gu, Wenqi Zhong, and Ke Gao. "Experimental Study on Co2 Co-Gasification Characteristics of Biomass and Waste Plastics: Insight into Interaction and Targeted Regulation Method." *Energy* 292 (2024). https://doi.org/10.1016/j.energy.2024.130509.

[15] Parrillo, Francesco, Filomena Ardolino, Carmine Boccia, Gabriele Calì, Davide Marotto, Alberto Pettinau, and Umberto Arena. "Co-Gasification of Plastics Waste and Biomass in a Pilot Scale Fluidized Bed Reactor." *Energy* 273 (2023). https://doi.org/10.1016/j.energy.2023.127220.

[16] Zulkafli, Aizatul Hikmah, Hamizura Hassan, Mohd Azmier Ahmad, Azam Taufik Mohd Din, and Siti Maryam Wasli. "Co-Pyrolysis of Biomass and Waste Plastics for Production of Chemicals and Liquid Fuel: A Review on the Role of Plastics and Catalyst Types." *Arabian Journal of Chemistry* 16, no. 1 (2023). https://doi.org/10.1016/j.arabjc.2022.104389.

[17] Mishra, Somya, and Rajesh Kumar Upadhyay. "Review on Biomass Gasification: Gasifiers, Gasifying Mediums, and Operational Parameters." *Materials Science for Energy Technologies* 4 (2021): 329-40. https://doi.org/10.1016/j.mset.2021.08.009.

[18] Schneider, Christoph, Michael Zeller, Daniel Böhm, and Thomas Kolb. "Influence of Pressure on the Gasification Kinetics of Two High-Temperature Beech Wood Chars with Co2, H2o and Its Mixture." *Fuel* 299 (2021). https://doi.org/10.1016/j.fuel.2021.120523.

[19] Sanjaya, Eric, and Ali Abbas. "Plasma Gasification as an Alternative Energy-from-Waste (Efw) Technology for the Circular Economy: An Environmental Review." *Resources, Conservation and Recycling* 189 (2023). https://doi.org/10.1016/j.resconrec.2022.106730.

[20] Hassan, H., J. K. Lim, and B. H. Hameed. "Catalytic Co-Pyrolysis of Sugarcane Bagasse and Waste High-Density Polyethylene over Faujasite-Type Zeolite." *Bioresour Technol* 284 (Jul 2019): 406-14. https://doi.org/10.1016/j.biortech.2019.03.137. https://www.ncbi.nlm.nih.gov/pubmed/30965196.

[21] Ocampo Batlle, Eric Alberto, York Castillo Santiago, Osvaldo José Venturini, José Carlos Escobar Palacio, Electo Eduardo Silva Lora, Diego Mauricio Yepes Maya, and Alberto Ricardo Albis Arrieta. "Thermodynamic and

Environmental Assessment of Different Scenarios for the Insertion of Pyrolysis Technology in Palm Oil Biorefineries." *Journal of Cleaner Production* 250 (2020). https://doi.org/10.1016/j.jclepro.2019.119544.

[22] Suriapparao, Dadi V., Dharavath Anil Kumar, and R. Vinu. "Microwave Co-Pyrolysis of Pet Bottle Waste and Rice Husk: Effect of Plastic Waste Loading on Product Formation." *Sustainable Energy Technologies and Assessments* 49 (2022). https://doi.org/10.1016/j.seta.2021.101781.

[23] Yousef, Samy, Justas Eimontas, Sharath P. Subadra, and Nerijus Striūgas. "Functionalization of Char Derived from Pyrolysis of Metallised Food Packaging Plastics Waste and Its Application as a Filler in Fiberglass/Epoxy Composites." *Process Safety and Environmental Protection* 147 (2021): 723-33. https://doi.org/10.1016/j.psep.2021.01.009.

[24] Francis Prashanth, P., M. Midhun Kumar, and R. Vinu. "Analytical and Microwave Pyrolysis of Empty Oil Palm Fruit Bunch: Kinetics and Product Characterization." *Bioresour Technol* 310 (Aug 2020): 123394. https://doi.org/10.1016/j.biortech.2020.123394. https://www.ncbi.nlm.nih.gov/pubmed/32361644.

[25] Atnaw, Samson Mekbib, Shaharin Anwar Sulaiman, and Suzana Yusup. "Syngas Production from Downdraft Gasification of Oil Palm Fronds." *Energy* 61 (2013): 491-501. https://doi.org/10.1016/j.energy.2013.09.039.